論文 / 著書情報
Article / Book Information

Title	Fusion of amyloid beta with ferritin yields an isolated oligomeric beta-sheet-rich aggregate inside the ferritin cage
Authors	Basudev Maity, Shiori Kameyama, Jiaxin Tian, Thuc Toan Pham, Satoshi Abe, Eri Chatani, Kazuyoshi Murata, Takafumi Ueno
Citation	Biomaterials Science, Vol. 12, Issue 9, Page 2408-2417
Pub. date	2024, 3
DOI	https://dx.doi.org/10.1039/d4bm00173g
Note	This file is author (final) version.

Fusion of amyloid beta with ferritin yields an isolated oligomeric beta-sheet-rich aggregate inside the ferritin cage

*Basudev Maity,[1] Shiori Kameyama,[1] Jiaxin Tian,[1] Thuc Toan Pham,[1] Satoshi Abe,[1] Eri Chatani,[2] Kazuyoshi Murata,[3,4] Takafumi Ueno[1,5]**

[1]School of Life Science and Technology, Tokyo Institute of Technology, Nagatsuta-cho 4259, Midori-ku, Yokohama 226 8501, Japan.

[2]Department of Chemistry, Graduate School of Science, Kobe University, Kobe, Hyogo 657-8501, Japan

[3]Exploratory Research Center on Life and Living Systems (ExCELLS), National Institute for Natural Sciences, Okazaki, Aichi, 444-8585, Japan.

[4]National Institute for Physiological Sciences (NIPS), National Institute for Natural Sciences, Okazaki, Aichi, 444-8585, Japan

[5] Living Systems Materialogy (LiSM) Research Group, International Research Frontiers Initiative (IRFI), Tokyo Institute of Technology, Nagatsuta-cho 4259, Midori-ku, Yokohama 226-8501, Japan

Keywords: Ferritin cage; Amyloid beta; β-sheet-rich oligomer; High-speed AFM.

Abstract

Alzheimer's disease is a severe brain condition caused by the formation of amyloid plaques composed of amyloid beta (Aβ) peptide. These peptides form oligomer, protofibril, and fibril before deposition into amyloid plaques. Among these intermediates, Aβ oligomers (AβO) were found to be the most toxic and therefore an appealing target for drug development and understanding their role in the disease. However, precise isolation and characterization of AβOs have proven challenging because AβOs tend to aggregate and form heterogeneous mixtures in solution. As a solution, we genetically fused the Aβ peptide with a ferritin monomer. Such fusion allowed to encapsulate precisely 24 Aβ peptides inside the 24-mer ferritin cage. Using high-speed atomic force microscopy (HS-AFM), we disassembled the ferritin and directly visualized the Aβ core enclosed within the cage. The thioflavin-T assay (ThT) and attenuated total reflection infrared spectroscopy (ATR-IR) reveal the presence of β-sheet structure in the encapsulated oligomeric aggregate. Gallic acid, an amyloid inhibitor can inhibit the fluorescence of ThT bounded AβO. Our approach represents a significant advance in the isolation and characterization of a β-sheet rich AβO and is expected to be useful for future studies of other disordered peptides such as α-synuclein and tau.

Introduction

Protein cages have gained significant attention in biomaterials science due to their well-defined capsule-like structures with monodisperse sizes.[1, 2] These cages are formed by self-assembly of protein monomers. Virus-like particles, ferritin, heat-shock proteins and chaperonins are typical examples of protein cages.[3] Such particles serve various purposes, such as templates for synthesizing nanomaterials, drug delivery vehicles, and catalytic reaction chambers.[4] Recently, it was found that larger biomolecules such as proteins and enzymes can be encapsulated within these cages without compromising their original functions.[5-8] Those reports suggests that the confined environment in protein cages can maintain the native folded state of the encapsulated biomolecules. Based on this understanding, we aimed to utilize protein cages to isolate and investigate the properties of disordered proteins, which are challenging to study in solution due to their tendency to form aggregates and deposits. In this work, we focused on isolating Aβ peptides into a typical host protein cage, ferritin and allow the encapsulated Aβ peptides to form oligomer inside the cage (Figure 1).

Amyloid β (Aβ) peptide is known to be involve in Alzheimer's disease (AD) which is a neurodegenerative disorder in mammals (Figure 1c).[9] These peptides readily oligomerize and form protofibril and fibril, which finally accumulate in pathogenic plaques.[10] Most of the current research on Aβ peptide primarily focuses on efforts to understand the molecular mechanisms behind Aβ oligomerization and fibril formation.[11] Studies have indicated that Aβ oligomers (AβOs) are the most toxic and pathogenic form of Aβ.[12-15] This makes AβOs an appealing target for developing oligomer-specific drugs, exploring their properties and roles in the disease, and understanding the mechanism of fibril formation.[15, 16]

However, analyzing AβOs in detail, including their dynamic features in solution, is challenging due to their transient nature, aggregation tendency, heterogeneity, and difficulties in isolating well-

defined oligomers.[17-20] Several strategies have been used to address these issues, such as encapsulating Aβ monomers into reverse micelles and promoting the formation of extended β-strands, which are believed to be the nuclei of fibril formation.[21, 22] Similarly, neurotoxic AβOs were prepared through disulfide bond formation.[23] High-speed atomic force microscopy (HS-AFM) has also been utilized to study Aβ peptide aggregation and fibril formation.[24] Another approach involves preparing AβOs through photo-crosslinking treatment to investigate their nanoscale dynamics.[25, 26] Computational studies have proposed that a crowded molecular environment can stabilize Aβ aggregation.[27] Therefore, if the AβOs are not protected, they become prone to aggregation over time and are more likely to enhance the aggregation at high concentration.

In this study, we aimed to isolate a defined number of Aβ monomers within a confined protein environment that allows them to interact freely and form oligomers. The use of a protein cage offers several advantages, including genetic fusion for precise encapsulation of Aβ monomers, prevention of aggregation of AβOs, and provision of pores on the cage surface which permit entry of small molecules to influence the oligomer properties. Considering these factors, we selected the ferritin protein cage as a suitable template for isolating a defined number of Aβ peptides.

Ferritin stands out among other protein cages due to its unique structural features and exceptional characteristics. It exhibits remarkable thermal stability at temperatures as high as 100°C and maintains its integrity over a broad pH range of 2 to 11.[28] The spherical ferritin cage is formed by self-assembly of 24 subunits, which creates an internal space with a diameter of 8 nm (Figure 1b). Since the C-terminal ends of the subunits are located inside the cage, a genetic fusion of Aβ at each of the C-terminal ends was expected to result in encapsulation of 24 peptides into the cage (Figure 1b and 1d).

Herein, we demonstrated the genetic fusion of Aβ42 at the C-terminal end of the ferritin cage to induce the formation of AβO within the restricted protein environment (Figure 1d). We have

chosen *E. coli* as the host for expressing Fr-Aβ42 monomers due to its widespread use in efficient recombinant protein expression and its ability to provide the necessary cellular environment for forming 24-mer ferritin cage assembly.[29] Transmission electron microscopy (TEM) analysis revealed that the ferritin cage containing Aβ42 forms a well-defined spherical cage structure rather than aggregating randomly. Using high-speed AFM (HS-AFM), we directly visualized the encapsulated Aβ core by disassembling the cage in solution. The Thioflavin-T (ThT) assay indicated the formation of AβO. The ThT-AβO complex can be inhibited by gallic acid, a typical amyloid inhibitor. Attenuated total reflectance-infrared spectroscopy (ATR-IR) measurements confirmed the β-sheet structures within the Aβ core. Previous efforts to study AβO in solution were challenged due to a lack of suitable methods to stop aggregation. Our methodology allows precise isolation of a defined β-sheet-rich oligomer fused with the protein cage, which can be used to conduct in-depth studies on the properties and behavior of AβOs.

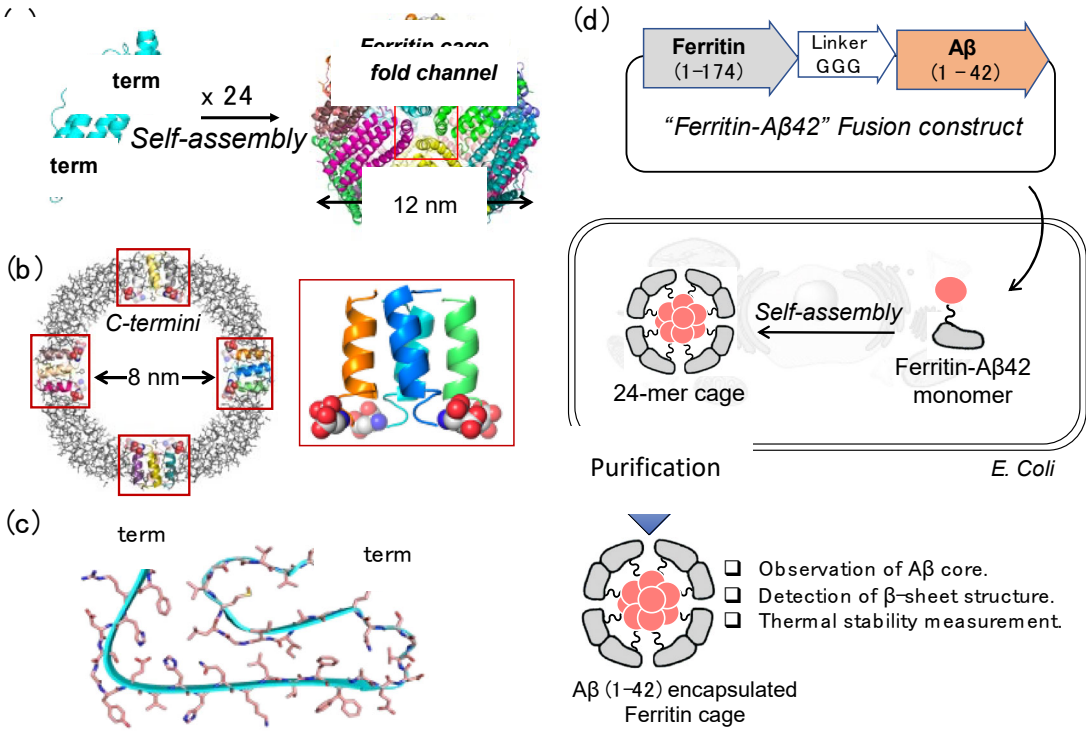

Figure 1: **In-cell packaging of a defined number of Aβ peptides fused with the ferritin cage monomer.** (a) Self-assembly of the 24 ferritin monomers to form a spherical cage structure showing the 4-fold symmetry facing forward (pdb: 1DAT). (b) Interior structure of the ferritin cage showing the position of E-helices (cartoon) and C-termini along with an expanded view of four E-helices. The C-terminal residue, Asp174 is shown with a sphere model. The selected square areas represent the positions of 4 E-helices at the 4-fold symmetric channels, with one of them shown in an enlarged view. (c) Monomeric structure of a typical Aβ peptide from a fibrillar structure (pdb: 6SZF). (d) Schematic illustration showing the genetic fusion of the Aβ peptide at the C-terminal end of the ferritin monomer through a flexible GGG linker and encapsulation of the fused peptides into the 24-mer cage during the assembly of the Fr-Aβ monomer inside the *E. Coli* cell.

Results

Design and in-cell packaging of Aβ peptides into the ferritin cage

Design and preparation

Recombinant horse spleen apo-ferritin (apo-rHLFr) was employed as a suitable template for encapsulating Aβ peptides because this ferritin can be expressed in high yield, easily crystallized and is very stable. The C-terminal end of apo-rHLFr (FrWT) is located inside the cage (Figure 1b). To enable free interaction among Aβ peptides and oligomer formation, we fused a full-length of Aβ peptide with 42 residues to FrWT with a GGG linker (Figure 1d and Table S1-3). During the expression of **Fr-Aβ42** monomer in *E. coli* cells and subsequent assembly formation, the 24 Aβ peptides can be encapsulated within the ferritin cage (**Fr-Aβ42** for 42 Aβ residues) (Figure 1d). The inherent tendency of Aβ peptides to interact with each other is likely involved during the encapsulation process. The resulting 24-mer ferritin cage was purified by cell disruption and heat treatment at 70°C for 15 minutes, followed by anion exchange and size exclusion chromatography (*see* supporting information). Although the protein expression level of **Fr-Aβ42** was found less compared to FrWT, we successfully isolated and purified the **Fr-Aβ42** containing Aβ in a sufficient yield for comprehensive characterization including protein crystallization (Figure S1a,b and Figure 1). The isolated yield of **Fr-Aβ42** per 1 g of cells was 0.1 mg, which is less than that of FrWT (9.5 mg). Other than low expression, the intrinsic aggregation nature of the Aβ, a section of **Fr-Aβ42** might not form the 24-mer cage which could attribute to the low recovery yield.

Characterization

Subsequently, the purified **Fr-Aβ42** was subjected to comprehensive spectral and analytical characterization. Native polyacrylamide gel electrophoresis (PAGE) analysis of **Fr-Aβ42** showed banding patterns similar to those of FrWT. This indicates that the fused Aβ peptides are effectively packed into the ferritin cage in *E. coli* without altering its original size (Figure 2a). This finding is

further supported by size exclusion chromatography (SEC), which revealed identical elution times for FrWT and **Fr-Aβ42** (Figure S1). The successful fusion of Aβ peptides within the ferritin cage was confirmed by the matrix-assisted laser desorption ionization time-of-flight mass spectrometric analysis (MALDI-TOF). The calculated mass for **Fr-Aβ42** is 24,513 Da, and the observed mass is 24,513 Da (Figure 2b). We also measured the zeta potential of both FrWT and Fr-Aβ42 which are -6.8 mV and -6.2 mV, respectively, which suggest that the surface properties of the ferritin cage remained same.

The hydrodynamic diameter based on volume percentages of FrWT and **Fr-Aβ42** measured by dynamic light scattering (DLS) were found to be 13.4 ± 1.4 and 13.4 ± 0.7 nm, respectively in 50 mM Tris-HCl (pH 8.0) / 0.15 M NaCl (Figure 2c). The transmission electron microscopic (TEM) analysis revealed spherical shapes of FrWT and **Fr-Aβ42** with diameters of 13.6 ± 0.9 and 13.7 ± 0.6 nm, respectively (Figure 2d and 2e). This suggests that the encapsulation of Aβ peptides does not cause a significant change in the size of the ferritin cage.

X-ray crystal structure analysis

To gain atomic-level insights into the structure, **Fr-Aβ42** was crystallized, and its structure was determined by X-ray crystallography at a resolution of 2.0 Å (Table S4). Although we modeled the overall ferritin cage structure, the Aβ core was left unmodelled due to insufficient electron density at the center of the cage (Figure S2). It is to be noted that, Aβ, being an inherently disordered peptide, lacks a fixed structure and that might be the reason for not observing any density of the fused Aβ peptide in the $2F_o$-F_c map. A similar phenomena was also previously observed when ferritin was fused with metal binding peptide which was not appeared in the crystal structure. [30, 31] The root mean square deviation (RMSD) of C_α atoms of the protein chain from that of FrWT (PDB ID: 1DAT) is only 0.183. This result provides further support for our interpretation that the fusion and encapsulation of Aβ peptides does not affect the overall ferritin cage structure. Notably, the

four E-helices of the **Fr-Aβ42** cage were observed in the usual position (Figure S2e). This suggests that the ferritin cage is folded into its native "flip" conformation in contrast to the "flop" conformation in which the E-helices are located outside the cage due to the fusion of long peptides (Table S5). This signifies that the fused Aβ peptide core is located inside the cage.

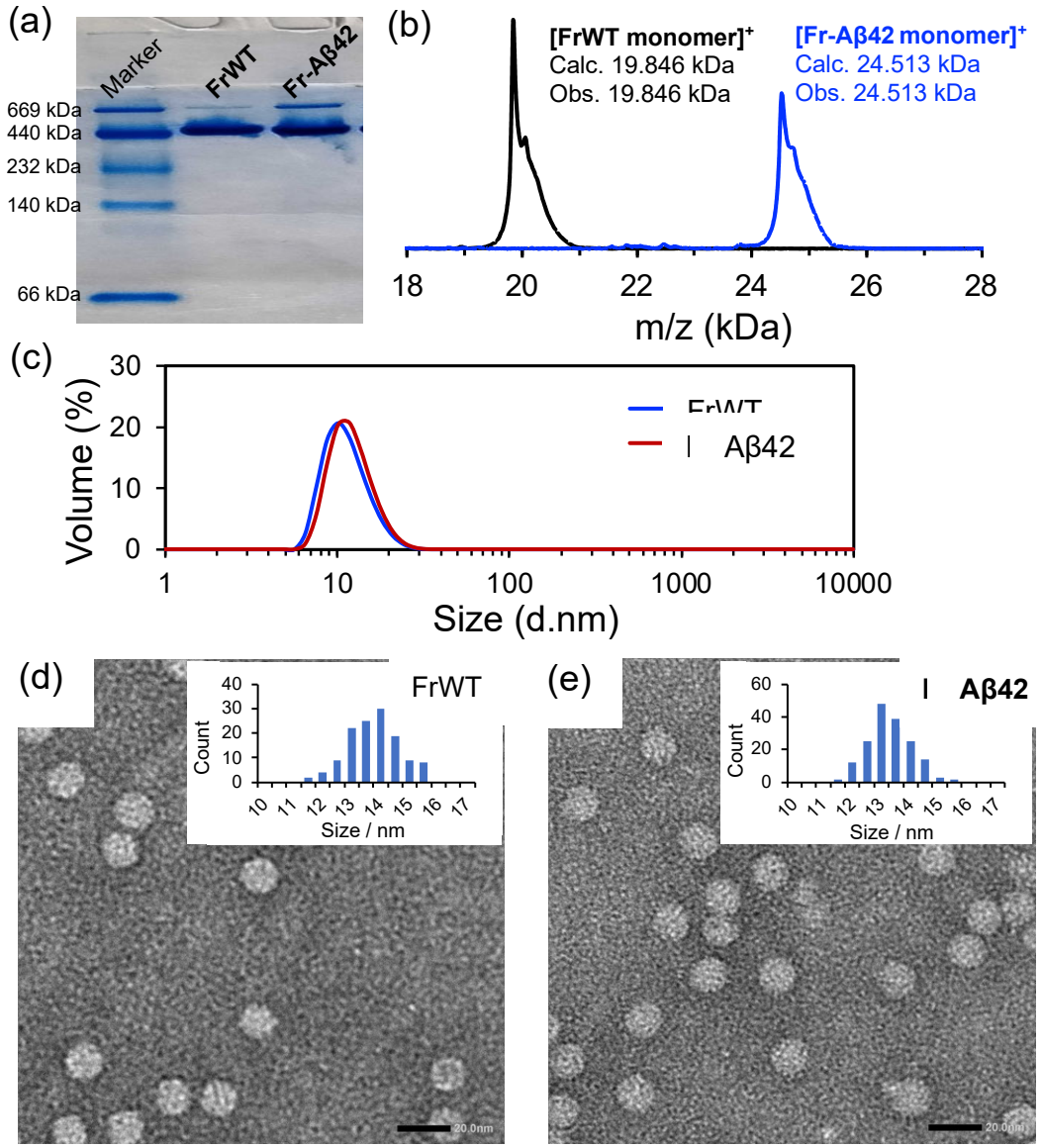

Figure 2: Characterization of the Aβ encapsulated ferritin cage, Fr-Aβ42. (a) Native polyacrylamide gel electrophoresis (PAGE) banding pattern of FrWT and **Fr-Aβ42**. (b) Matrix-assisted laser desorption ionization time-of-flight mass spectrometric analysis (MALDI-TOF) mass of FrWT and **Fr-Aβ42** monomer. (c) Hydrodynamic diameter of FrWT and **Fr-Aβ42** in 50 mM Tris-HCl (pH 8) / 0.15 M NaCl. (d-e) Transmission emission microscopy (TEM) images showing the spherical shape of FrWT and **Fr-Aβ42**. Staining: 1 min in 1% Methyl amine tungstate (Nanoprobes). Scale bar: 20 nm.

Visualization of the encapsulated Aβ peptides by high-speed AFM (HS-AFM)

After successfully isolating and characterizing **Fr-Aβ42**, we aimed to visualize the encapsulated AβO by HS-AFM, which is a powerful tool for investigating the dynamics of protein structures.[24] Visualizing the AβO core directly is challenging because it is located inside the ferritin cage and covered by the protein shell (Figure 2e). To overcome this issue, we disassembled the ferritin cage during the HS-AFM measurement to visualize the AβO.[32]

To facilitate the disassembly process, we conducted HS-AFM measurements at pH 2.3 (50 mM Gly-HCl / 0.1 M KCl), as the ferritin cage is known to start disassembling at lower pH levels.[33] At first, we focused on a single **Fr-Aβ42** cage and captured snapshots of it at various intervals until disassembly occurred. Figure 3a and Figure S3 with selected HS-AFM snapshots (Movie 1 and Movie 2) present two examples of the dynamic disassembly of a single **Fr-Aβ42** cage. The HS-AFM movie 1 revealed that after 6.3 sec (Figure 3a), the spherical structure of the **Fr-Aβ42** cage collapses and exposes the Aβ core into the buffer at 6.9 sec. At 12s, the amyloid core, surrounded by disassembled ferritin subunits, becomes clearly visible, producing a flower-like shape with a central core (Figure 3a, Movie 1). Such a unique shape was not observed for the FrWT (Figure 3b and Movie 3).

The height distribution profile of one of the typical flower-like structures indicates that the height of the amyloid core is higher than that of the surrounding ferritin subunits (Figure 3c). The average size of the disassembled **Fr-Aβ42** cage, including the amyloid core surrounded by the ferritin subunit, is 28 nm, which is nearly double that of an intact ferritin cage (Figure 3c). At this pH, various types of Aβ core were observed in the solution. The average height of the amyloid core is 7.7 nm (Figure 3c and 3d) in comparison to height of ferritin subunits which is approximately 4 nm (Figure 3c). The ferritin cage is usually 12 nm in size, but when it disassembles at a low pH, the subunits drift apart and lose their globular shape.[33] The disassembled ferritin subunits in **Fr-**

Aβ42 generate the distinctive flower-like structure, allowing the amyloid core to remain in its oligomeric configuration through Aβ-Aβ interactions.

Monitoring an amyloid core in the flower-like structure over time, we observed dynamic changes in its shape, which indicate a transition from globular to linear/deformed and then to globular again (Figure 3e, Figure S5, Movie 4 and Movie 5). This feature is consistent with the typical behavior of AβO, which was previously shown to be dynamic in nature and undergo shape alterations from globular to linear.[25]

Due to the restricted cage size, the encapsulated AβO might not exhibit dynamic behavior and maintain a globular shape. However, after disassembling the ferritin cage, the amyloid core became exposed to the solution and became dynamic. Notably, the disassembled ferritin subunits prevent the amyloid core from aggregating, which allowed us to characterize its dynamic nature in solution.

We need to mention that, although we visualized the encapsulated AβO by HS-AFM, the biological and atomic level properties of the AβO might differ from those found in Alzhaimer's disease patient as the measurement was done under acidic conditions (pH 2.3). Nevertheless, HS-AFM is the only method that enables direct visualization of the globular shape and the dynamic nature of AβO exposed from the ferritin cage. This approach overcame the challenge of directly visualizing the core and provided important insights into the dynamic nature of AβO. In the flower-like structure, the amyloid core is wrapped by the fused ferritin subunits. This demonstrates that due to Aβ-Aβ interaction, the oligomeric state remained intact, otherwise it would have been drift apart as shown in Figure 3b.

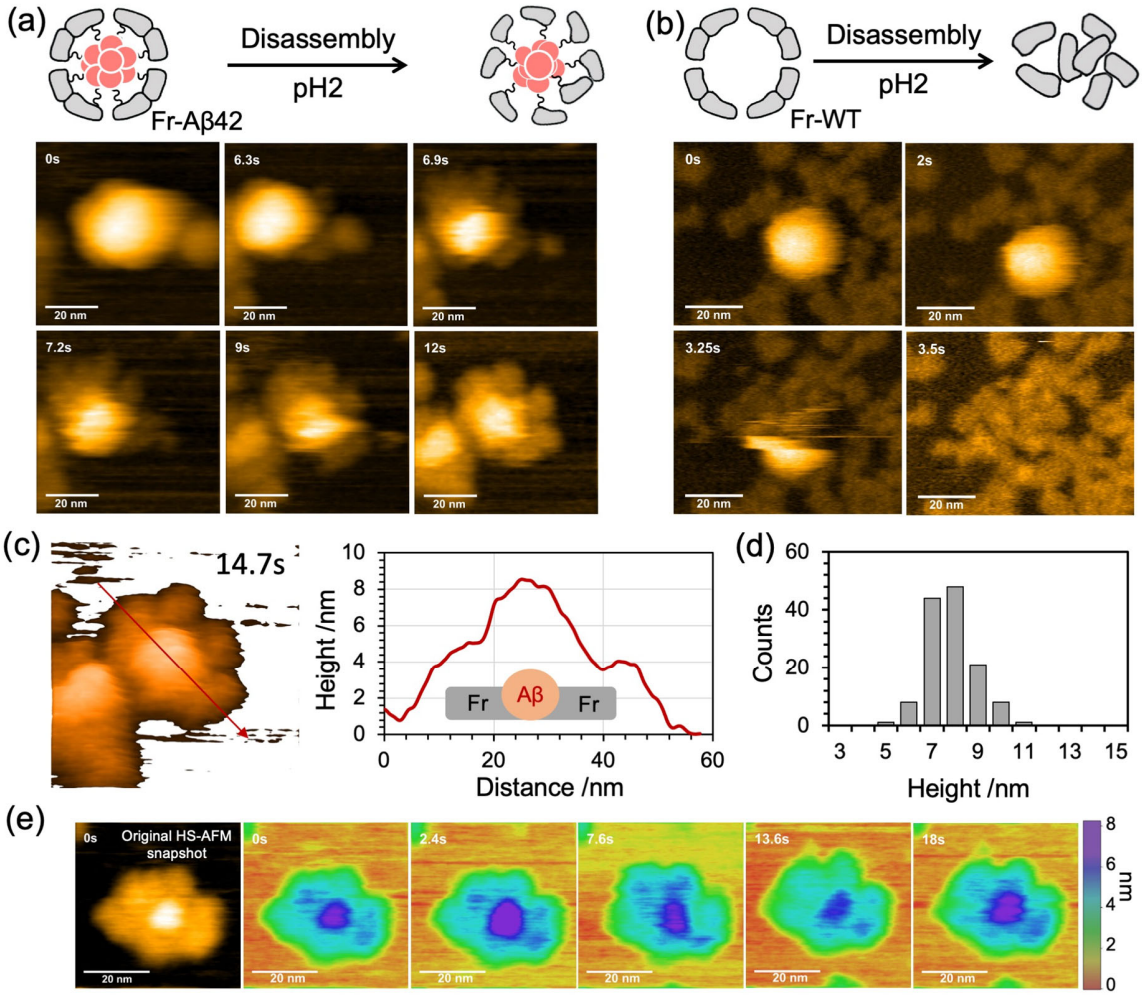

Figure 3: **Visualization of Aβ core by high-speed AFM (HS-AFM)**. (a) HS-AFM snapshots of the dynamic observation of a single molecule **Fr-Aβ42** in pH 2.3 (50 mM Gly-HCl-100 mM KCl). (b) HS-AFM snapshots of the disassembly of FrWT under similar condition as for **Fr-Aβ42**. (c) Three-dimensional image of a HS-AFM snapshot (14.7s) of the disassembly of **Fr-Aβ42** and the corresponding height profile analysis. The height profile was measured along the red arrow. (d) The height distribution profile of the Aβ cores obtained after the disassembly of **Fr-Aβ42** at pH2.3. (e) Heat-plot showing the time-dependent dynamic structural changes of a flower-like structure overtime. The purple color indicates highest height corresponding to the Aβ core which changed with time.

Evidence of β-sheet-rich amyloid core in Fr-Aβ42.

Thioflavin T (ThT) assay

We conducted a ThT assay to explore the secondary structure of **Fr-Aβ42**.[34, 35] ThT is a nonfluorescent dye that exhibits blue fluorescence upon specific binding to β-sheet structures. Ferritin cage consists of 8 symmetric three-fold channels (Figure S2b) through which large molecules like Zn-phthalocyanine (Approx. size: 15.7 Å x 15.7 Å; CCDC No. 1013162) can enter into the cage simply by incubating at room temperature.[36] Therefore, being smaller in size in comparison to Zn-phthalocyanine, ThT dye (14.1 Å x 4.6 Å ; CCDC No. 1816441) is expected to enter into the cage and binds to β-sheet structure if present. The **Fr-Aβ42** solution, when incubated with ThT, shows a strong fluorescence band at 480 nm, while no fluorescence is observed for FrWT under similar experimental conditions (Figure 4a). This finding suggests the presence of β-sheet structures in **Fr-Aβ42** and the formation of an oligomer inside the ferritin cage.

To confirm that the observed ThT fluorescence in our assay was not due to ThT self-aggregation or other phenomena in solution, size exclusion chromatography was performed using an incubated mixture of ThT and **Fr-Aβ42** (Figure 4b). Protein absorbance at 280 nm and ThT fluorescence (FL) at 480 nm were monitored simultaneously. No fluorescence peak was observed in the elution profile of FrWT (Figure 4b(i)). In contrast, **Fr-Aβ42** showed coexistence of UV and FL peaks in the elution profile at 10 min. This indicates that the ThT fluorescence originates from the ferritin cage containing Aβ core.

Attenuated total reflectance infrared spectroscopy (ATR-IR) measurement

For further verification of the presence of a β-sheet in the ferritin cage, we obtained ATR-IR spectroscopy measurements. The spectrum exhibit the characteristic IR stretching frequency near 1630 cm^{-1} corresponding to the extended parallel β-stranded structure (Figure 4c).[37, 38] This

frequency appears as a shoulder to the amide-I stretching frequency at 1650 cm^{-1} and is more prominent in the second derivative plot (Figure 4c(ii)). Importantly, FrWT does not show such a peak. This supports the presence of a β-sheet rich AβO inside **Fr-Aβ42**. The observed amyloid β-sheet structure is likely to exist in parallel in nature because the Aβ peptide is fused at the C-terminal end of each of four parallel E-helices.

Overall, the ThT assay and ATR-IR results demonstrate the presence of β-sheet structures in the encapsulated oligomeric Aβ aggregates inside the ferritin cage.

Gallic acid (GA) inhibition assay

Inhibition of fibrilization of Aβ peptides is known to occur in the presence various organic substances including polyphenolic compounds, such as gallic acid which is known to interact with the fibrillar Aβ structure .[39-41] In order to test whether the encapsulated oligomeric β-sheet-rich Aβ aggregate inside ferritin cage has any such effect, we chose gallic acid as a starting model inhibitor. Gallic acid was added during ThT assay and the fluorescence peak at 480 nm was monitored with time (Figure 4d). It was found that high gallic acid concentration leads to more decrease in the ThT fluorescence. The ThT fluorescence intensity at 480 nm was found to decrease over time at a particular inhibitor concentration. Since the rate of gallic acid oxidation is faster in alkaline pH, a control experiment at pH 6.8 was performed which also showed inhibition of ThT fluorescence at 480 nm but at a slower rate (Figure S6). These results indicate that the gallic acid inhibitor interacts with the β-sheet rich AβO inside the cage and possibly induces structural changes in the ThT-bounded Aβ core which lead to the release of ThT as well as ThT fluorescence. We observed a new peak appearing at 510 nm after significance decrease in ThT fluorescence (Figure S6). This suggests possible formation of a structure with different fluorescence properties involving gallic acid after the ThT inhibition because ThT florescence is specific at 480 nm.[39]

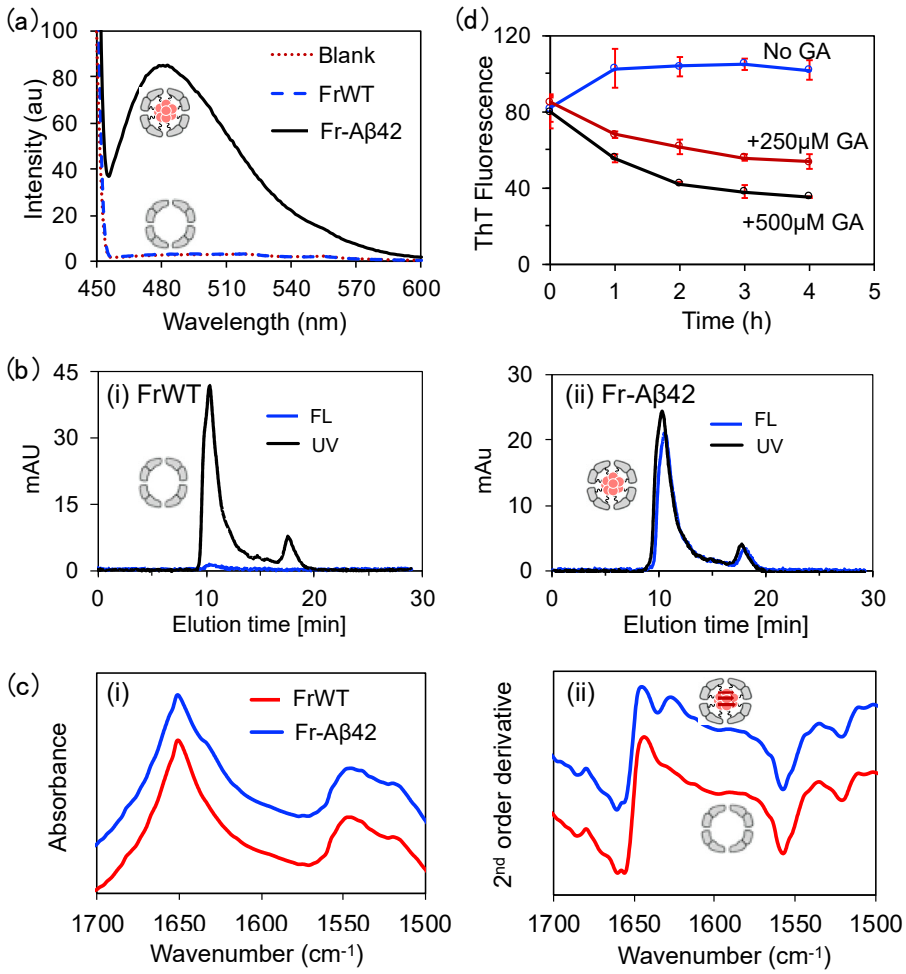

Figure 4: **Evaluation of the β-sheet structure in Fr-Aβ42**. (a) Thioflavin-T (ThT) assay showing the appearance of the fluorescence band at 480 nm for **Fr-Aβ42**. 10 μM of ThT and 1 μM of protein in 50 mM Tris-HCl (pH 8.0) /0.15 M NaCl was used for the study. (b) Size exclusion chromatography of the mixtures used for ThT assay showing the coexistence of both UV and ThT fluorescence (FL) in the elution profile of FrWT (i) and **Fr-Aβ42** (ii). Elution buffer: 20 mM Tris-HCl. Flow: 0.5 ml/min. (c) Attenuated Total Reflectance Infrared spectroscopy (ATR-IR) spectra of FrWT and **Fr-Aβ42** (i) and the corresponding second order derivative plot (ii). The spectra of FrWT and **Fr-Aβ42** are shown as red and blue lines, respectively. (d) Effect on ThT fluorescence at 480 nm over time after addition of gallic acid (250 μM and 500 μM) into **Fr-Aβ42** solution (10 μM ThT and 1 μM protein in 50 mM Tris-HCl (pH 8.0 /0.15 M NaCl. The error bar represents standard deviations from three independent experiments.

Thermal stability measurement of the Aβ encapsulated ferritin cage by circular dichroism (CD) spectroscopy

CD measurements were carried out to investigate the changes in secondary structure observed upon heating (Figure 5). At 25°C, FrWT and **Fr-Aβ42** show the characteristic negative bands at 208 nm and 222 nm corresponding to the α-helix structure (Figure 5a and 5b). Although the presence β-sheet structure was indicated by ThT assay, no distinct absorption band was observed for the β-sheet structure near 215 nm in the CD spectrum of **Fr-Aβ42** (Figure 5a and 5b). The secondary structure analysis from the CD spectrum of **Fr- Aβ42** indicates the presence of only 4% of β-sheet structure (Table S6). This suggests that **Fr-Aβ42** has a predominant α-helix structure. When the temperature was raised gradually from 25°C to 100°C, the molar ellipticity of FrWT at 222 nm (θ_{222}) slightly increased, and the CD spectrum after cooling down to RT remained almost identical to the original CD spectrum (Figure 5a). This suggests that FrWT remains stable at 100°C. **Fr-Aβ42** showed a different pattern in which the $(\theta)_{222}$ increased slightly up to 85°C in a manner similar to the pattern of FrWT and then increased sharply up to 100°C (Figure 5c and 5d). This suggests that **Fr-Aβ42** starts denaturing after 85°C (Figure 5d) by losing its secondary structures as reflected in the CD spectrum in Figure 5b and Table S6. In HS-AFM measurement, we found that the AβO is dynamic in nature (Figure 3e and Figure S5), higher temperature likely enhanced their dynamic behavior and impact on the cage stability. As a result, the **Fr-Aβ42** denatured at high temperature which was not observed for FrWT.

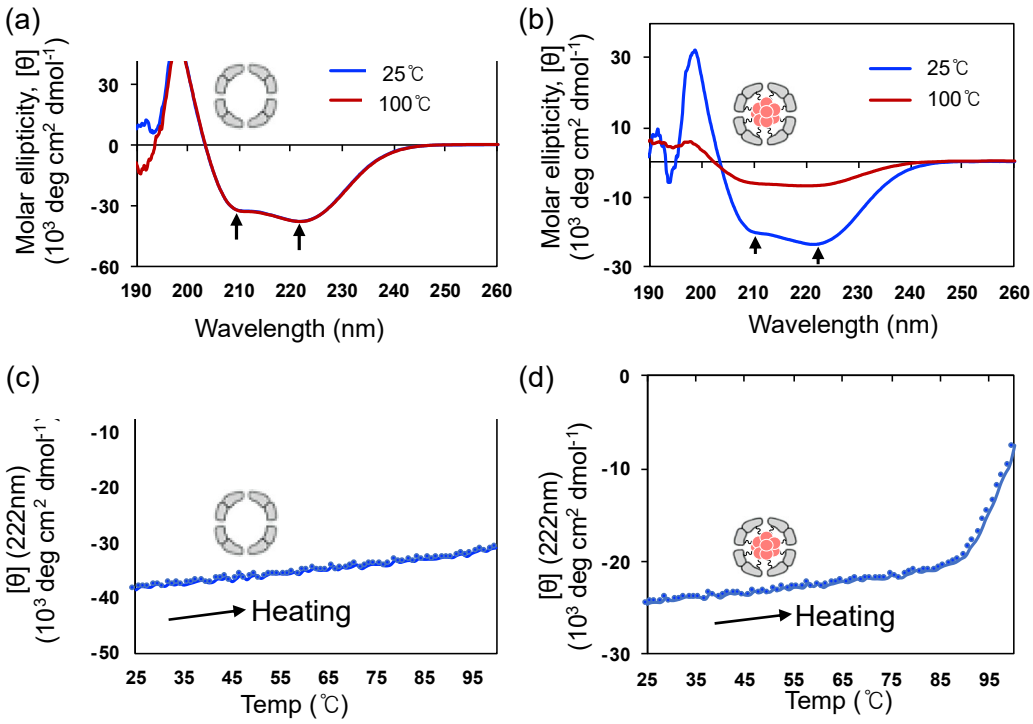

Figure 5: **Measurement of thermal stability of Fr-Aβ42 by Circular dichroism (CD) spectroscopy.** CD spectra measured at 25°C before heating and after heating at 100°C for (a) FrWT and (b) **Fr-Aβ42**. The arrows indicate the positions of alpha-helix peaks at 208 nm and 222 nm. Changes of molar ellipticity at 222 nm, $(\theta)_{222}$ during heating from 25°C to 100°C with a temperature gradient of 1°C min^{-1} for (c) FrWT and (d) **Fr-Aβ42**. Measurements were done with a protein concentration of 0.1 mg/ml in 50 mM Tris-HCl (pH 8) /0.15 M NaCl.

Discussions

In this study, we successfully isolated a precisely defined number of Aβ peptides by fusing them into a self-assembled ferritin cage. Since the self-assembly process occurs inside the cell, one can expect that the Aβ-Aβ interaction and formation of oligomeric aggregate inside the ferritin cage is more natural than the same if occur in buffer solution outside the cell. It is important to note that although the fused Aβ peptides freely interact with each other inside the cage, the characteristic of the formed oligomeric aggregates might not be the exact same as occurred in Alzhaimer's disease due to fusion. Nevertheless, our method of encapsulation of a fused AβO inside the ferritin cage is valuable for understanding their nature, structure, and properties as they are intrinsically disorder in nature and difficult to isolate. The restricted environment of the ferritin cage helps AβO to avoid mutual aggregation and preserve the oligomeric nature of the amyloid core encapsulated within the cage. Previous attempts using reverse micelles to isolate AβOs showed less stability and onset of aggregation over time.[22] In our case, the AβO inside the ferritin cage remained stable over time (Figure S1c). As Aβ oligomers are considered the most toxic species in Alzheimer's disease (AD), our approach is useful for studying the properties, toxicity, and disease-related roles of a precisely defined isolated AβO.

It should be noted that retrieving the encapsulated AβO out of the cage could be beneficial for studying oligomer-oligomer interaction that give rise to protofibrils or fibrils, etc. However, it is challenging to retrieve them because the AβO is fused to the ferritin monomer, and the cage can only disassemble at an extremely acidic pH (<2.0). Our intention was not to conduct those studies because such investigations can be easily carried out using Aβ peptides in a solution.[18, 24, 42] Rather, we focused on a method to inhibit the oligomer-oligomer aggregation, which is a common problem in studying isolated single oligomers.

The fusion of foreign proteins and peptides at the C-terminal end of the ferritin cage is not new (Table S5). Such fusion does not cause any changes in the spherical shape of the ferritin cage. However, fusion of proteins with over 28 residues causes shifting of the E-helix towards the outside of the cage (Table S5). Notably, in our case, the strong aggregation propensity of Aβ peptides which include 42 residues is anticipated to play a crucial role in their encapsulation into the cage (Figure 1d). Interestingly, the encapsulated 24-mer AβO falls in the category of toxic high molecular weight (HMW) oligomers which could be targets for drug discovery.[43, 44]

The Aβ peptide encapsulated ferritin cage was found to be highly stable up to 85 ℃, although not comparable with FrWT which denatured over 100 ℃. The inherent disordered nature of the Aβ peptide was considered to be the reason for less stability of **Fr-Aβ42** than FrWT.[45] This is reflected in the CD spectrum (Figure 5d). Since low temperature (70 ℃) was used to denature the impurities during the **Fr-Aβ42** purification, protein loss due to stability issue might be less. Other than thermal stability, no noticeable changes in the physicochemical properties was observed. The 24-mer cage integrity was maintained up to pH2.3 similar to FrWT while the zeta potential and the overall cage size remained same.

Another intriguing aspect of our study is the visualization of Aβ core by HS-AFM and dynamic changes in shape with time. Such dynamic features indicate that it might be an intermediate of higher order assembly formation such as fibril. Therefore, targeting this type of AβO could stop formation of fibril.

Conclusions

In conclusion, we have successfully demonstrated a novel method for isolating a single β-sheet-rich AβO within a ferritin cage. This was achieved by fusing the N-terminal of the Aβ peptide

to the C-terminal ends of subunits of ferritin. Due to such fusion, when the 24-mer ferritin cage is formed, 24 Aβ peptides are encapsulated into the cage. The Aβ encapsulated ferritin cage has a spherical cage structure similar to that of FrWT. The encapsulated Aβ peptide core inside ferritin was directly visualized by HS-AFM after disassembling the cage. By ThT assay and ATR-IR, we confirmed the presence of a β-sheet structure in the encapsulated Aβ core. The ThT bounded Aβ core was affected by an amyloid inhibitor, gallic acid. The **Fr-Aβ42** cage was found to be stable even at 85℃. The isolation of a single AβO through our fusion method holds significant potential for advancing our understanding of the structure, properties, and dynamics of AβOs. Since small molecules such as gallic acid and ThT can enter the cage, our method could be a handy way to figure out if an oligomer-targeting drug is worth exploring further. The method is useful for other proteins related to disorders. The exceptional cage stability can be a secure storage space for AβO with an inherent tendency to aggregate. Looking at the big picture, one could use cleavable linkers to engineer the ferritin cage for therapeutic peptide delivery. Furthermore, our approach may have broader applications beyond drug discovery, specifically in studying other intrinsically disordered proteins (IDPs), such as α-synuclein and tau, which are challenging to analyze because they are prone to forming aggregates in solution.

Abbreviations

Aβ, Amyloid beta ; AD, Alzhaimer's Disease; AβO, Amyloid beta oligomer; ATR-IR, Attenuated total reflectance-Fourier transform infrared spectroscopy; CD, Circular Dichroism; FrWT, Ferritin wildtype; Fr-Aβ42, Ferritin cage containing 24 Aβ peptides with 42 residues; FL, Fluorescence; HS-AFM, High-Speed Atomic Force Microscopy; HMW, High molecular weight; IDP, Intrinsically disordered protein; rHLFr, Recombinant horse spleen L-ferritin; MALDI-TOF, matrix-assisted laser desorption ionization time-of-flight mass spectrometric mass analysis; PAGE,

Polyacrylamide gel electrophoresis; RMSD, Root mean square deviation; SEC, Size exclusion chromatography; TEM, Transmission Emission Microscopy; ThT, Thioflavin T.

Author Contributions

The manuscript was written through contributions of all authors. All authors have given approval to the final version of the manuscript.

Funding Sources

This work was supported by "JSPS KAKENHI" (Grant No. 22H00347 to T. Ueno; 19K15695, 22H04744 and 20H05438 to B. Maity) and "Grant-in-Aid for Scientific Research on Innovative Areas 'Molecular Engines' (Grant No. JP18H05421 to T. Ueno) from Ministry of Education, Culture, Sports, Science and Technology.

Acknowledgment

We thank Prof. Sam Yong Park and Prof. Kenji Mizutani from Yokohama City University for their help in initial X-ray diffraction measurements of **Fr-Aβ42**. We are also thankful to Prof. T. Uchihashi lab for initial stage of HS-AFM measurements. We thank Mr. Y. Nakasuji for SAXS measurements. We also thank OFC Bio Division for DNA sequencing and X-ray diffraction (XtaLAB Synergy-DW-FS-OFC), MALDI-TOF at Tokyo Institute of Technology. We also thank Dr. Yoko Kayama of NIPS for the collection and processing of TEM images.

References

(1) Bhaskar, S.; Lim, S. Engineering protein nanocages as carriers for biomedical applications. *NPG Asia Mater.* **2017**, *9* (4), e371-e371. DOI: 10.1038/am.2016.128.

(2) Zhang, Y.; Ardejani, M. S.; Orner, B. P. Design and Applications of Protein-Cage-Based Nanomaterials. *Chem. Asian J.* **2016**, *11* (20), 2814-2828. DOI: https://doi.org/10.1002/asia.201600769.

(3) Aumiller, W. M.; Uchida, M.; Douglas, T. Protein cage assembly across multiple length scales. *Chem. Soc. Rev.* **2018**, *47* (10), 3433-3469, 10.1039/C7CS00818J. DOI: 10.1039/C7CS00818J.

(4) Edwardson, T. G. W.; Levasseur, M. D.; Tetter, S.; Steinauer, A.; Hori, M.; Hilvert, D. Protein Cages: From Fundamentals to Advanced Applications. *Chem. Rev.* **2022**. DOI: 10.1021/acs.chemrev.1c00877.

(5) Hestericová, M.; Heinisch, T.; Lenz, M.; Ward, T. R. Ferritin encapsulation of artificial metalloenzymes: engineering a tertiary coordination sphere for an artificial transfer hydrogenase. *Dalton Trans.* **2018**, *47* (32), 10837-10841, 10.1039/C8DT02224K. DOI: 10.1039/C8DT02224K.

(6) Tetter, S.; Hilvert, D. Enzyme Encapsulation by a Ferritin Cage. *Angew. Chem. Int. Ed.* **2017**, *56* (47), 14933-14936. DOI: https://doi.org/10.1002/anie.201708530.

(7) Patterson, D. P.; Prevelige, P. E.; Douglas, T. Nanoreactors by Programmed Enzyme Encapsulation Inside the Capsid of the Bacteriophage P22. *ACS Nano* **2012**, *6* (6), 5000-5009. DOI: 10.1021/nn300545z.

(8) Patterson, D. P.; Schwarz, B.; Waters, R. S.; Gedeon, T.; Douglas, T. Encapsulation of an Enzyme Cascade within the Bacteriophage P22 Virus-Like Particle. *ACS Chemical Biology* **2014**, *9* (2), 359-365. DOI: 10.1021/cb4006529.

(9) Murphy, M. P.; LeVine Iii, H. Alzheimer's Disease and the Amyloid-β Peptide. *J. Alzheimer's Dis.* **2010**, *19*, 311-323. DOI: 10.3233/JAD-2010-1221.

(10) Barz, B.; Liao, Q.; Strodel, B. Pathways of Amyloid-β Aggregation Depend on Oligomer Shape. *J. Am. Chem. Soc.* **2018**, *140* (1), 319-327. DOI: 10.1021/jacs.7b10343.

(11) Lee, S. J. C.; Nam, E.; Lee, H. J.; Savelieff, M. G.; Lim, M. H. Towards an understanding of amyloid-β oligomers: characterization, toxicity mechanisms, and inhibitors. *Chem. Soc. Rev.* **2017**, *46* (2), 310-323, 10.1039/C6CS00731G. DOI: 10.1039/C6CS00731G.

(12) Sengupta, U.; Nilson, A. N.; Kayed, R. The Role of Amyloid-β Oligomers in Toxicity, Propagation, and Immunotherapy. *EBioMedicine* **2016**, *6*, 42-49. DOI: https://doi.org/10.1016/j.ebiom.2016.03.035.

(13) Kayed, R.; Head, E.; Thompson, J. L.; McIntire, T. M.; Milton, S. C.; Cotman, C. W.; Glabe, C. G. Common Structure of Soluble Amyloid Oligomers Implies Common Mechanism of Pathogenesis. *Science* **2003**, *300* (5618), 486-489. DOI: doi:10.1126/science.1079469.

(14) Yankner, B. A.; Lu, T. Amyloid β-Protein Toxicity and the Pathogenesis of Alzheimer Disease*. *J. Biol. Chem.* **2009**, *284* (8), 4755-4759. DOI: https://doi.org/10.1074/jbc.R800018200.

(15) Ono, K.; Condron, M. M.; Teplow, D. B. Structure–neurotoxicity relationships of amyloid β-protein oligomers. *Proc. Natl. Acad. Sci. U.S.A.* **2009**, *106* (35), 14745-14750. DOI: doi:10.1073/pnas.0905127106.

(16) Sakono, M.; Zako, T. Amyloid oligomers: formation and toxicity of Aβ oligomers. *FEBS J.* **2010**, *277* (6), 1348-1358. DOI: https://doi.org/10.1111/j.1742-4658.2010.07568.x.

(17) Parodi-Rullán, R.; Ghiso, J.; Cabrera, E.; Rostagno, A.; Fossati, S. Alzheimer's amyloid β heterogeneous species differentially affect brain endothelial cell viability, blood-brain barrier integrity, and angiogenesis. *Aging Cell* **2020**, *19* (11), e13258. DOI: https://doi.org/10.1111/acel.13258.

(18) Meng, F.; Yoo, J.; Chung, H. S. Single-molecule fluorescence imaging and deep learning reveal highly heterogeneous aggregation of amyloid-β 42. *Proc. Natl. Acad. Sci. U.S.A.* **2022**, *119* (12), e2116736119. DOI: doi:10.1073/pnas.2116736119.

(19) Hubin, E.; van Nuland, N. A. J.; Broersen, K.; Pauwels, K. Transient dynamics of Aβ contribute to toxicity in Alzheimer's disease. *Cellular and Molecular Life Sciences* **2014**, *71* (18), 3507-3521. DOI: 10.1007/s00018-014-1634-z.

(20) Cline, E. N.; Bicca, M. A.; Viola, K. L.; Klein, W. L. The Amyloid-β Oligomer Hypothesis: Beginning of the Third Decade. *J. Alzheimer's Dis.* **2018**, *64*, S567-S610. DOI: 10.3233/JAD-179941.

(21) Eskici, G.; Axelsen, P. H. Amyloid Beta Peptide Folding in Reverse Micelles. *J. Am. Chem. Soc.* **2017**, *139* (28), 9566-9575. DOI: 10.1021/jacs.7b03333.

(22) Lin, Y.-L.; Cheng, Y.-S.; Ho, C.-I.; Guo, Z.-H.; Huang, S.-J.; Org, M.-L.; Oss, A.; Samoson, A.; Chan, J. C. C. Preparation of fibril nuclei of beta-amyloid peptides in reverse micelles. *Chem. Commun.* **2018**, *54* (74), 10459-10462, 10.1039/C8CC05882B. DOI: 10.1039/C8CC05882B.

(23) Sandberg, A.; Luheshi, L. M.; Söllvander, S.; Pereira de Barros, T.; Macao, B.; Knowles, T. P. J.; Biverstål, H.; Lendel, C.; Ekholm-Petterson, F.; Dubnovitsky, A.; et al. Stabilization of neurotoxic Alzheimer amyloid-β oligomers by protein engineering. *Proc. Natl. Acad. Sci. U.S.A.* **2010**, *107* (35), 15595-15600. DOI: doi:10.1073/pnas.1001740107.

(24) Watanabe-Nakayama, T.; Ono, K.; Itami, M.; Takahashi, R.; Teplow, D. B.; Yamada, M. High-speed atomic force microscopy reveals structural dynamics of amyloid β_{1–42} aggregates. *Proc. Natl. Acad. Sci. U.S.A.* **2016**, *113* (21), 5835-5840. DOI: 10.1073/pnas.1524807113.

(25) Banerjee, S.; Sun, Z.; Hayden, E. Y.; Teplow, D. B.; Lyubchenko, Y. L. Nanoscale Dynamics of Amyloid β-42 Oligomers As Revealed by High-Speed Atomic Force Microscopy. *ACS Nano* **2017**, *11* (12), 12202-12209. DOI: 10.1021/acsnano.7b05434.

(26) Yamin, G.; Huynh, T.-P. V.; Teplow, D. B. Design and Characterization of Chemically Stabilized Aβ42 Oligomers. *Biochemistry* **2015**, *54* (34), 5315-5321. DOI: 10.1021/acs.biochem.5b00318.

(27) Yeung, P. S. W.; Axelsen, P. H. The Crowded Environment of a Reverse Micelle Induces the Formation of β-Strand Seed Structures for Nucleating Amyloid Fibril Formation. *J. Am. Chem. Soc.* **2012**, *134* (14), 6061-6063. DOI: 10.1021/ja3004478.

(28) Hishikawa, Y.; Noya, H.; Nagatoishi, S.; Yoshidome, T.; Maity, B.; Tsumoto, K.; Abe, S.; Ueno, T. Elucidating Conformational Dynamics and Thermostability of Designed Aromatic Clusters by Using Protein Cages. *Chemistry – A European Journal n/a* (n/a), e202300488. DOI: https://doi.org/10.1002/chem.202300488.

(29) Carrondo, M. A. Ferritins, iron uptake and storage from the bacterioferritin viewpoint. *The EMBO Journal* **2003**, *22* (9), 1959-1968. DOI: https://doi.org/10.1093/emboj/cdg215.

(30) Calisti, L.; Trabuco, M. C.; Boffi, A.; Testi, C.; Montemiglio, L. C.; des Georges, A.; Benni, I.; Ilari, A.; Taciak, B.; Białasek, M.; et al. Engineered ferritin for lanthanide binding. *PloS one* **2018**, *13* (8), e0201859. DOI: 10.1371/journal.pone.0201859.

(31) Davidov, G.; Abelya, G.; Zalk, R.; Izbicki, B.; Shaibi, S.; Spektor, L.; Shagidov, D.; Meyron-Holtz, E. G.; Zarivach, R.; Frank, G. A. Folding of an Intrinsically Disordered Iron-Binding Peptide in Response to Sedimentation Revealed by Cryo-EM. *Journal of the American Chemical Society* **2020**, *142* (46), 19551-19557. DOI: 10.1021/jacs.0c07565.

(32) Kim, M.; Rho, Y.; Jin, K. S.; Ahn, B.; Jung, S.; Kim, H.; Ree, M. pH-Dependent Structures of Ferritin and Apoferritin in Solution: Disassembly and Reassembly. *Biomacromolecules* **2011**, *12* (5), 1629-1640. DOI: 10.1021/bm200026v.

(33) Maity, B.; Li, Z.; Niwase, K.; Ganser, C.; Furuta, T.; Uchihashi, T.; Lu, D.; Ueno, T. Single-molecule level dynamic observation of disassembly of the apo-ferritin cage in solution. *Physical Chemistry Chemical Physics* **2020**, *22* (33), 18562-18572, 10.1039/D0CP02069A. DOI: 10.1039/D0CP02069A.

(34) Xue, C.; Lin, T. Y.; Chang, D.; Guo, Z. Thioflavin T as an amyloid dye: fibril quantification, optimal concentration and effect on aggregation. *Royal Society Open Science* **2017**, *4* (1), 160696. DOI: doi:10.1098/rsos.160696.

(35) Younan, N. D.; Viles, J. H. A Comparison of Three Fluorophores for the Detection of Amyloid Fibers and Prefibrillar Oligomeric Assemblies. ThT (Thioflavin T); ANS (1-Anilinonaphthalene-8-sulfonic Acid); and bisANS (4,4′-Dianilino-1,1′-binaphthyl-5,5′-disulfonic Acid). *Biochemistry* **2015**, *54* (28), 4297-4306. DOI: 10.1021/acs.biochem.5b00309.

(36) Zhen, Z.; Tang, W.; Guo, C.; Chen, H.; Lin, X.; Liu, G.; Fei, B.; Chen, X.; Xu, B.; Xie, J. Ferritin Nanocages To Encapsulate and Deliver Photosensitizers for Efficient Photodynamic Therapy against Cancer. *ACS Nano* **2013**, *7* (8), 6988-6996. DOI: 10.1021/nn402199g.

(37) Sarroukh, R.; Goormaghtigh, E.; Ruysschaert, J.-M.; Raussens, V. ATR-FTIR: A "rejuvenated" tool to investigate amyloid proteins. *Biochimica et Biophysica Acta (BBA) - Biomembranes* **2013**, *1828* (10), 2328-2338. DOI: https://doi.org/10.1016/j.bbamem.2013.04.012.

(38) Moran, S. D.; Zanni, M. T. How to Get Insight into Amyloid Structure and Formation from Infrared Spectroscopy. *J. Phys. Chem. Lett.* **2014**, *5* (11), 1984-1993. DOI: 10.1021/jz500794d.

(39) Yu, M.; Chen, X.; Liu, J.; Ma, Q.; Zhuo, Z.; Chen, H.; Zhou, L.; Yang, S.; Zheng, L.; Ning, C.; et al. Gallic acid disruption of Aβ1–42 aggregation rescues cognitive decline of APP/PS1 double transgenic mouse. *Neurobiology of Disease* **2019**, *124*, 67-80. DOI: https://doi.org/10.1016/j.nbd.2018.11.009.

(40) Sakalauskas, A.; Ziaunys, M.; Smirnovas, V. Gallic acid oxidation products alter the formation pathway of insulin amyloid fibrils. *Scientific Reports* **2020**, *10* (1), 14466. DOI: 10.1038/s41598-020-70982-3.

(41) LeVine, H., III; Lampe, L.; Abdelmoti, L.; Augelli-Szafran, C. E. Dihydroxybenzoic Acid Isomers Differentially Dissociate Soluble Biotinyl-Aβ(1–42) Oligomers. *Biochemistry* **2012**, *51* (1), 307-315. DOI: 10.1021/bi201288x.

(42) Morel, B.; Carrasco, M. P.; Jurado, S.; Marco, C.; Conejero-Lara, F. Dynamic micellar oligomers of amyloid beta peptides play a crucial role in their aggregation mechanisms. *Physical Chemistry Chemical Physics* **2018**, *20* (31), 20597-20614, 10.1039/C8CP02685H. DOI: 10.1039/C8CP02685H.

(43) Yuan, M.; Tang, X.; Han, W. Anatomy and formation mechanisms of early amyloid-β oligomers with lateral branching: graph network analysis on large-scale simulations. *Chemical Science* **2022**, *13* (9), 2649-2660, 10.1039/D1SC06337E. DOI: 10.1039/D1SC06337E.

(44) Shea, D.; Daggett, V. Amyloid-β Oligomers: Multiple Moving Targets. *Biophysica* **2022**, *2* (2), 91-110.

(45) Meng, F.; Bellaiche, M. M. J.; Kim, J.-Y.; Zerze, G. H.; Best, R. B.; Chung, H. S. Highly Disordered Amyloid-β Monomer Probed by Single-Molecule FRET and MD Simulation. *Biophys. J.* **2018**, *114* (4), 870-884. DOI: https://doi.org/10.1016/j.bpj.2017.12.025.